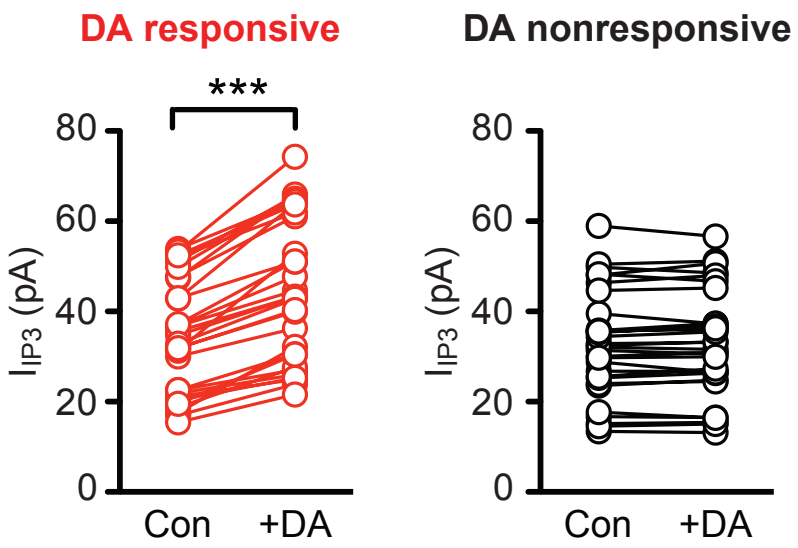

Figure S1 (related to Figure 1). Graphs plotting I_{IP3} amplitude in control and with preceding DA application in two subpopulations of MSNs illustrated in Figure 1C.

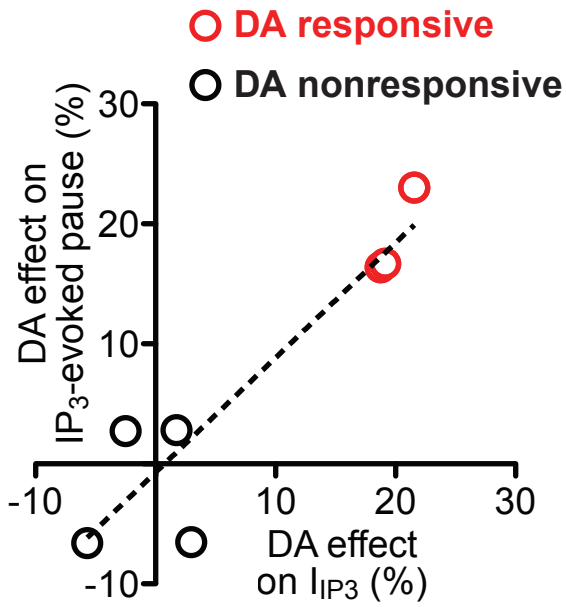

Figure S2 (related to Figure 2). The magnitude of DA effect on I_{IP3}-evoked firing pauses assessed in current clamp is plotted versus the magnitude of DA effect on I_{IP3} measured in voltage clamp in individual MSNs. Dashed line is a linear fit to all data points ($r = 0.92$, $p < 0.01$; Pearson correlation).

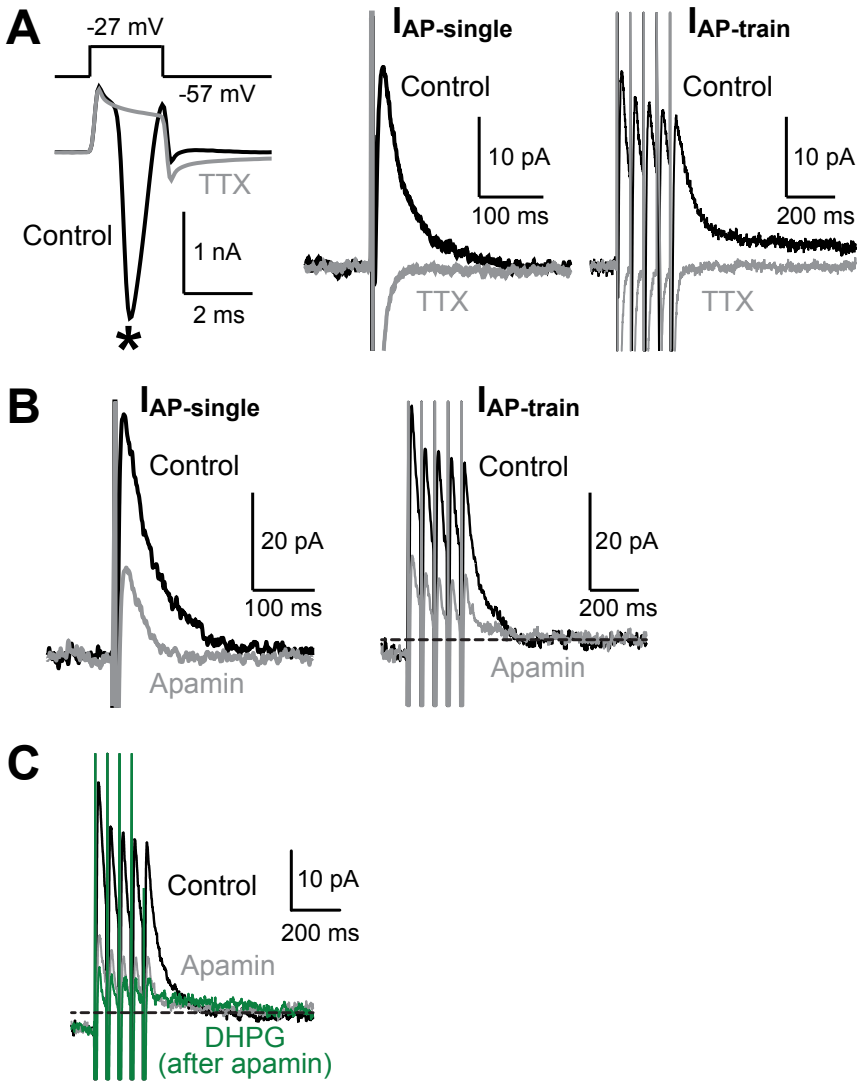

Figure S3 (related to Figure 3). (A) Example traces showing that TTX (1 μM), which blocked the unclamped AP-dependent transient inward current (asterisk in the left trace) during the 2 ms depolarization, abolished $I_{AP\text{-}single}$ and $I_{AP\text{-}train}$. (B) Example traces depicting the effect of apamin (100 nM) on $I_{AP\text{-}single}$ and $I_{AP\text{-}train}$. (C) Representative traces showing that DHPG failed to affect $I_{AP\text{-}train}$ after apamine treatment.

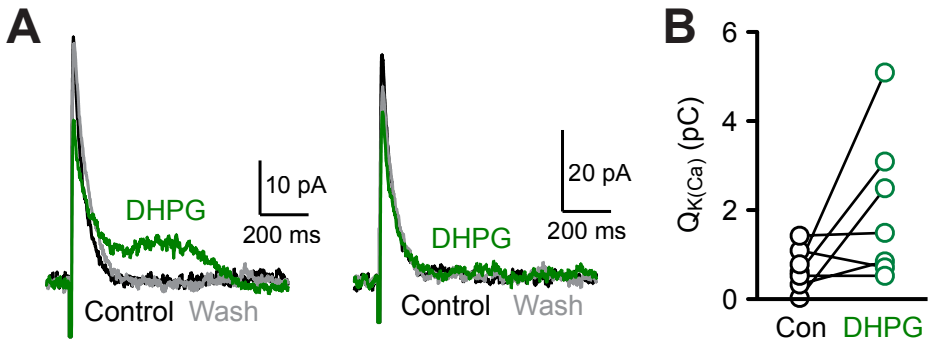

Figure S4 (related to Figure 3). (A) Example traces illustrating the effect of DHPG (5 μM) on $I_{AP\text{-}single}$ in two MSNs. Note that DHPG facilitated $I_{AP\text{-}single}$ in one cell (left), while having no effect in the other cell (right). (B) Summary graph showing DHPG effect on $Q_{K(Ca)}$ for

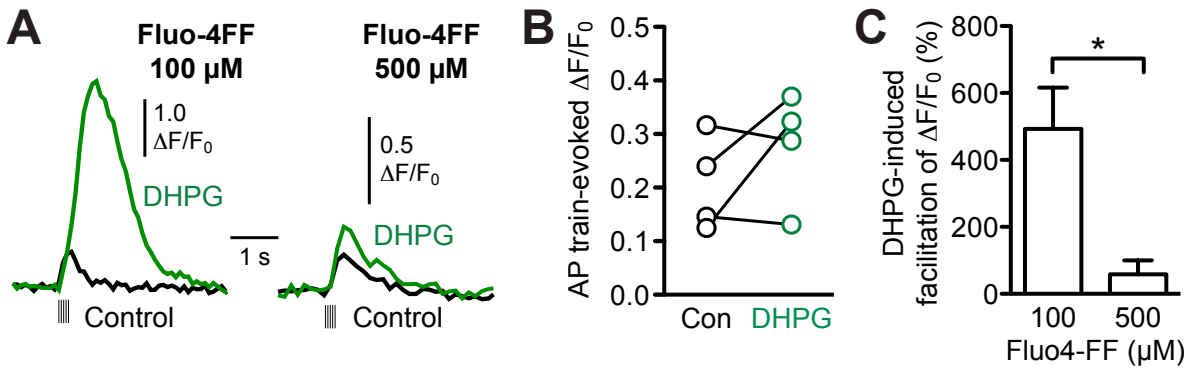

Figure S5 (related to Figure 3). (A) Example traces illustrating DHPG-induced facilitation of AP train-evoked Ca^{2+} transients monitored with 100 µM Fluo-4FF (left; from the same cell shown in Figure 4B) or 500 µM Fluo-4FF (right). (B) Plot of AP train-evoked Ca^{2+} transients (monitored with 500 µM Fluo-4FF) in control solution and in DHPG (5 µM) in 4 cells. (C) Summary bar graph showing that increasing Fluo-4FF concentration to 500 µM greatly reduced the DHPG effect on AP train-evoked Ca^{2+} transients (100 µM: n = 5 cells, 500 µM: n = 4 cells). *$p < 0.05$ (unpaired t test).